scientific reports

Check for updates

OPEN

# Investigation the adsorption mechanisms, chemical resistance and mechanical strength of the synthesized chitosan/activated carbon composite in methylene blue removal

Fatemeh Ebrahimzadeh & Ali Akbari✉

**This study is based on a new approach to the development of the adsorption process from two perspectives, including the possibility of using the adsorbent in a wide range of pH (increasing chemical resistance) and also its easy separation from solution (mechanical strength), or in other words the possibility of preparing a simple fixed bed for the adsorbent during adsorption process. According to this view, chitosan/activated carbon composite was synthesized and used to remove of methylene blue as a cationic pollutant from water. The structural properties of the synthesized adsorbent were analyzed using FE-SEM, FTIR, BET and zeta potential analyses, which showed significant improvement in chemical and physical stability. The influence of main parameters such as adsorbent dose, contact time, initial concentration and pH value of the solution in the adsorption process was investigated. The results showed that if chitosan is used more than half amount of carbon, the performance of the adsorbent decreases, which may be related to the filling of carbon pores by chitosan. According to the zeta potential analysis, the pH of point zero charge of the adsorbent was found to be 4.4. Also, the adsorption mechanism followed the Langmuir model and pseudo-second-order kinetics, and the maximum adsorption capacity of a single layer for methylene blue dye was measured 22.52 mg/g.**

**Keywords** Adsorption, Methylene blue pollutant, Activated carbon, Chitosan

Water pollution from a variety of dyes is a significant environmental concern. This form of pollution is primarily attributed to the textile industry and other related sectors such as printing, paper, paint, and leather production[1,2]. These organic compounds possess potential toxicity, carcinogenicity and resistance to biodegradation, rendering them hazardous environmental pollutants[3].

Methylene blue (MB), an organic dye and pigment, is a positively charged heterocyclic molecule with the chemical formula $C_{16}H_{18}N_3SCl$. This dark green powder, which turns water blue at room temperature and adsorbs visible light around 665 nm, is widely used as a coloring agent in industries such as pharmaceuticals, plastics, tanning, cosmetics, paper, food, and textiles. However, its use can lead to adverse effects including irritation of skin, mouth, throat, stomach, esophageal, as well as nausea, digestive pains, headache, diarrhea, vomiting, fever, dizziness, and high blood pressure. Improper disposal of waste containing this dye can also have severe environmental consequences[4]. Among various treatment techniques, adsorption stands out as a highly promising technology extensively employed for the elimination of hazardous pollutants from wastewater[5].

Activated carbon is known as a suitable adsorbent for dye removal due to its cost-effectiveness, environmental compatibility, large specific surface area, adjustable porosity and abundant functional groups. However, the adsorption properties of activated carbon depend on its functional groups, which are mainly obtained from the activation processes, precursors and thermal treatment[6,7].

In the recent years, development of bio-based adsorbents has surged, for removal of water contaminants. In this regard, Negarestani et al. has conducted comprehensive studies on the use of natural adsorbents, such

Chemical Engineering Faculty, Sahand University of Technology, Tabriz, Iran. ✉email: ali_akbari@sut.ac.ir

as cotton fiber[8], sisal fiber[9] and luffa fiber[10] which confirmed the ability of bio-based adsorbents to water decolorization and removal of pharmaceutical contaminant.

Chitosan, a cost-effective cationic biopolymer derived from natural sources, has garnered significant attention for its unique properties, including high adsorption capacity, abundance, and affordability, setting it apart from other commercial adsorbents. Its insolubility in water, alkaline solutions, and organic solvents is attributed to the presence of hydrogen bonds between its molecules, while its solubility in acidic solutions is due to the protonation of its amine groups. These characteristics make chitosan a promising candidate for the adsorption of pollutants such as heavy metals and dyes, owing to its multiple functional groups[11].

The effectiveness of activated carbon and chitosan individually in removing dyes and heavy metals from industrial wastewater depending on pH is affected by their low adsorption capacity, chemical resistance and also mechanical strength. In fact, the pulverization of activated carbon especially under agitation during process, as well as the dissolution of chitosan in acidic solutions, challenges the separation of each of these adsorbents after the adsorption process.

The main objective of this work is to develop chitosan/activated carbon (CH/AC) composite, aiming to combine mechanical stability, adsorption performance, and chemical resistance across a broad pH range for methylene blue removal. Therefore, chitosan was coated on activated carbon modified with $H_3PO_4$ as a chemical activation reagent. In addition, $H_3PO_4$ facilitates the formation of acidic functional groups such as carboxyl, phenolic hydroxyl groups and lactones. The synthesis of the chitosan/activated carbon composite not only preserves the advantageous properties of both adsorbents, but also significantly reduces their respective disadvantages.

Several experiments including FTIR, BET, FE-SEM and Zeta potential tests were used to characterize the synthesized composites. Also, the influence of several important factors on the removal of MB dye as an organic pollutant under various conditions was investigated.

## Materials and methods

### Materials

Industrial grade granular activated carbon prepared from walnut shell was used as adsorbent base. Chitosan (CH) medium with a deacetylation degree of more than 80% was obtained from Azin Turkan Company. Coating of AC with CH was carried out using acetic acid and NaOH purchased from Merck. MB and HCl, purchased from Merck.

### Material preparation

*Preparation of activated carbon*

The carbon granules were washed several times with distilled water to remove impurities and dried in an oven at 100 °C for 12 h. Then impregnation procedure was carried out by soaking dried carbon granules in phosphoric acid solution (45% wt.). The activation process lasted for a period of 24 h, with $H_3PO_4$: AC impregnation ratios of 2:1(AC-2), 3:1(AC-3), and 4:1(AC-4). The obtained granules were subjected to heat treatment in an oven at 700 °C for 1 h. After heat treatment, it was washed with 10% HCl to remove ash, and then washed several times with hot distilled water to remove excess acid. The washed sample was dried at 110 °C to obtain the final product[12,13].

*Preparation of chitosan gel*

A certain amount of CH was mixed in 100 mL of 2% (v/v) concentrated acetic acid under constant stirring at 300 rpm for 3 h using a magnetic stirrer to obtain a homogeneous mixture[14].

*Preparation of chitosan/activated carbon composite*

About 2 g of acid-modified carbon was slowly added to the chitosan gel and stirred at room temperature for 20 h. The CH/AC composite was prepared by dropping the gel mixture into 0.7 M NaOH precipitation bath. After 3 h, the obtained granules were filtered and washed several times with distilled water to neutral pH and dried in an oven at 60 °C[15].

### Adsorbent characterization

A Fourier transform infrared spectrometer (FTIR, Burker Tensor 27, Germany) was used to assess the surface chemistry of synthesized composite in the range of 400–4000 $cm^{-1}$ before adsorption. The specific surface area and pore structure were determined using a Brunauer-Emmett-Teller device (BELSORP MINI II, Japan). The microstructure of the sorbent was characterized by physical adsorption/desorption of nitrogen at − 196 °C. The samples were analyzed using an elemental analyzer and based on differences in nitrogen content. The morphologies of the samples were observed using a scanning electron microscopy (MIRA3 FE-SEM, Czech Republic). Zeta potential test (Ztasizer Advanced Lab blue, England) was performed to investigate the surface charge of the synthesized adsorbents at different pH values. To prepare the samples before the test, 0.001 g of each sample was dissolved in 10 mL distilled water and then placed in an ultrasonic device for 5 min.

### Adsorption experiments

A series of batch experiments were conducted to examine the adsorption of MB on CH/AC composite. Experiments involved the use of containers containing 50 mL of MB dye solution with initial concentrations ranging from 10 to 100 mg/L. Different amounts of CH/AC (0.02–0.13 g) were introduced into the 50 ml colored solution at different pH values (3–9). These samples were stirred using an orbital shaker at a speed of 300 rpm for varying lengths of time (10–90 min) at ambient temperature. The adsorbents were then separated from the solution and the final MB concentration in the solution was determined using a UV-visible spectrophotometer

(Jenway 6705 UV/Vis, England) at a wavelength of 665 nm. The removal efficiency of MB by CH/AC and the equilibrium adsorption capacities $q_e$ (mg $g^{-1}$) of MB were calculated using Eqs. (1) and (2), respectively.

$$Removal\ (\%) = \frac{C_0 - C_e}{C_0} \times 100 \tag{1}$$

$$q_e = \left(\frac{C_0 - C_e}{m}\right) \times v \tag{2}$$

where $C_o$ and $C_e$ (ppm) are the initial and equilibrium concentrations of MB solutions, respectively. v was the volume of the solution in liter and m was the mass of the adsorbent used (g). All the adsorption experiments were replicated at least two times and an average of values was reported.

*Equilibrium study*

Adsorption isotherm is an equation used to determine the amount of pollutant adsorbed on the adsorbent surface at equilibrium concentration and constant temperature. Isotherm studies are crucial to know how the active sites of adsorbents are distributed, to optimize the use of adsorbents. In addition, the isotherm provides information about the maximum adsorption capacity of the adsorbent. In this study, Freundlich and Langmuir equilibrium isotherm models were used to describe adsorption data in batch mode. 50 ml of solution containing MB in concentrations of 10, 20, 30, 40, 50, 60 and 100 ppm were prepared. 0.1 g adsorbent was added to the prepared solutions. The solutions were stirred for 1 h and after separation of the adsorbents, the equilibrium concentrations of the solutions were measured as Ce. The obtained adsorption data were fitted with the isotherm models. The values of the isotherm correlation coefficients ($R^2$) provide information about which isotherm follows the experimental data better. The Langmuir model assumes that adsorption occurs in a monolayer formation, based on the assumption that the surface of the adsorbent contains active sites with uniform energy levels. Consequently, the energy associated with adsorption remains constant and the adsorbent surface has a finite number of sites that can interact and bind to the adsorbed species. Once all available sites are occupied, the adsorption process is limited to a monolayer as no further adsorption can take place. At this point the amount of adsorbate reaches its maximum capacity. Langmuir adsorption isotherm is expressed as follow:

$$q_e = \frac{q_m K_L C_e}{1 + K_L C_e} \tag{3}$$

where qe (mg/g) is the adsorption capacity at equilibrium, $q_m$ (mg/g) is the maximum MB adsorption capacity of CH/AC, and $K_L$ (L/mg) is the constant related to the rate of adsorption.

Freundlich isotherm is one of the most widely used isotherms in the explanation of adsorption equilibrium because it is considered as an empirical equation. In addition, the Freundlich model assumes that the surface energy of the adsorbent is inhomogeneous. Hence, stronger binding sites are occupied first, and as the degree of site occupation increases, the binding strength decreases[16]. The following equation defines the Freundlich isotherm:

$$q_e = K_F C_e^{1/n} \tag{4}$$

where $K_F$ and 1/n are the Freundlich equilibrium constant and exponent, respectively.

*Kinetics study*

Kinetic study helps researchers better understand the possible adsorption mechanism and reaction pathways. The kinetic model deals with the influence of observable parameters on the overall speed. To investigate kinetic adsorption, 50 ml of MB solution with an initial concentration of 30 ppm was taken and 0.1 g of adsorbent was added to the sample. The solutions were stirred for different time intervals from 10 to 90 min at room temperature; and after the completion of the time of each experiment, the final concentration of pollutants was measured. In the present work, pseudo-first-order (PFO) and pseudo-second-order (PSO) kinetic models were used to investigate the adsorption kinetics[17]. The nonlinear form of the PFO and PSO models are shown as Eqs. (5) and (6), respectively:

$$q_t = q_e(1 - e^{K_1 t}) \tag{5}$$

$$q_t = \frac{q_e^2\ K_2 t}{(1 + q_e K_2 t)} \tag{6}$$

where $q_e$ (mg/g) is the adsorption capacity at equilibrium, $q_t$ (mg/g) is the adsorbed amount of pollutant, $K_1$ ($min^{-1}$) and $K_2$ (g $mg^{-1}$ $min^{-1}$) are the PFO and PSO kinetics rate constants, respectively, and t (min) is the contact time.

## Resistance and stability of the synthesized adsorbent

To determine the mechanical strength of the adsorbents, MB adsorption test was taken under the following conditions: initial concentration of 30 ppm, adsorbent dose of 0.05 g, and time of 60 min. At the end of the tests, the adsorbents were separated from the adsorption medium using a centrifuge, washed with distilled water and dried in an oven at 100 °C. The dried samples were weighed, and the percentage of adsorbent crushing after the adsorption process was calculated for each sample.

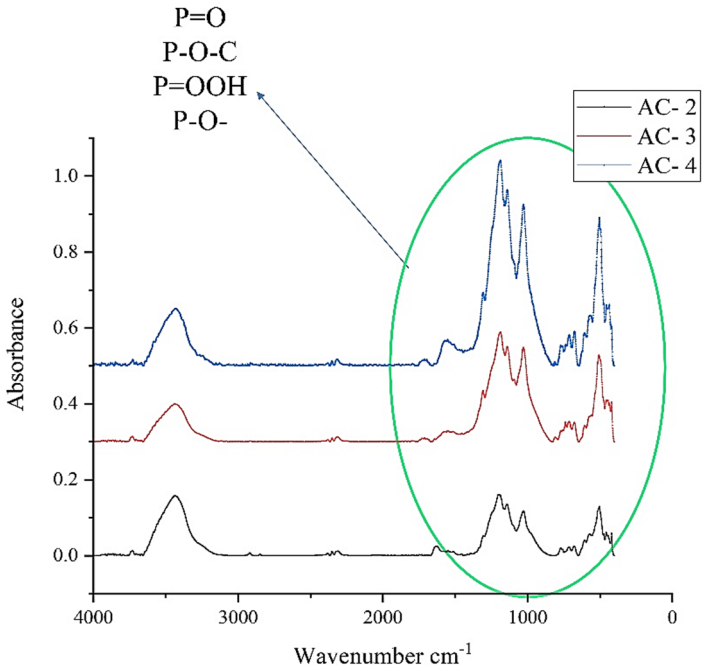


**Fig. 1**. FTIR spectra of modified carbon samples with different acid percentages.

| Sample | Impregnation ratio | Removal efficiency (%) |
|---|---|---|
| AC | 2 | 78.72 |
| | 3 | 83.00 |
| | 4 | 90.40 |

**Table 1**. Effect of phosphoric acid impregnation ratio on MB removal by ACs (initial MB concentration = 30 ppm, contact time = 30 min, dose = 0.05 g, shaking speed = 300 rpm, and temperature = 25 °C).

## Results and discussion

### Selection of adsorbent: effect of phosphoric acid impregnation ratio

FTIR spectra of the modified carbon samples with different acid contents are shown in Fig. 1. The obtained peaks are similar for all samples. However, as the saturation ratio (acid concentration) increases, the intensity of peaks in the range of 1000 to 1200 $cm^{-1}$ also increases. These peaks are attributed to the O–P stretching mode of the hydrogen bond, O–C stretching vibrations in the P–O–C (aromatic) bonds, and P–OOH bonds.

To investigate the impact of acid concentration during carbon modification on the adsorption of MB, three 50 ml solutions of MB dye were prepared with an initial concentration of 30 ppm. The adsorption test was conducted at neutral pH using 0.05 g of each adsorbent sample over a 30-minute period, and the obtained results are presented in Table 1.

The rise in acid concentration during carbon modification leads to an increase in acidic functional groups. Presence of these groups enhances the hydrophilicity of ACs and promotes their interaction with the MB molecules through the formation of hydrogen bonds, electrostatic attraction, and other interactions, leading to increase in the adsorption capacity of the adsorbent[18]. However, the decrease in the stability of AC granules (turn into powder) at acid impregnation ratios higher than 2, limited the use of high acid doses. This means that after the adsorption process, a centrifuge should be used to separate the adsorbent, which defeats the purpose of the project. Therefore, the saturation ratio of 2 was selected as the optimal acid concentration ratio for carbon modification.

### Selection of adsorbent: effect of chitosan presence on the removal of MB

The concentration ratio of chitosan to carbon was investigated as an important parameter in the composite synthesis process. To evaluate the performance of synthesized composites with different chitosan concentrations, MB adsorption test was carried out with an initial concentration of 30 ppm in 60 min and an adsorbent dose of 0.05 g. As shown in Fig. 2, it can be seen that by increasing the concentration ratio to 0.5, the adsorption capacity of MB increased and then decreased, which may be related to the filling of carbon pores by chitosan.

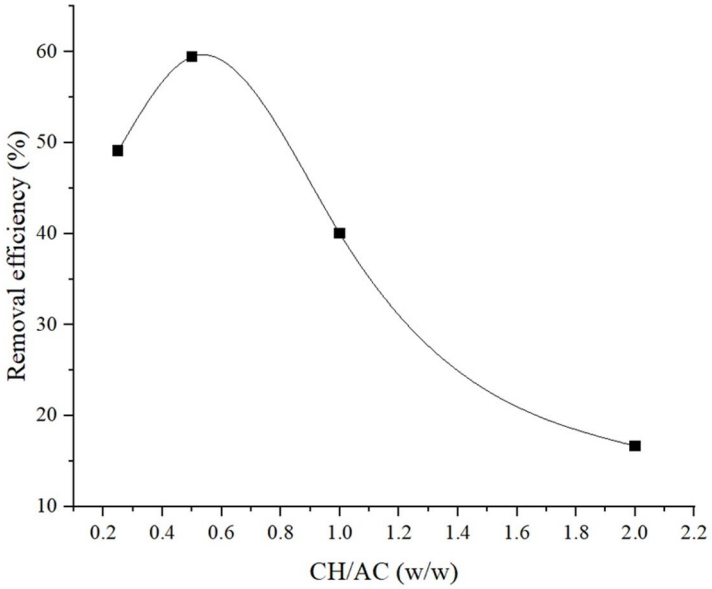


**Fig. 2**. Effect of chitosan presence on the composite for MB removal (initial MB concentration = 30 ppm, contact time = 60 min, dose = 0.1 g, shaking speed = 300 rpm, and temperature = 25 °C).

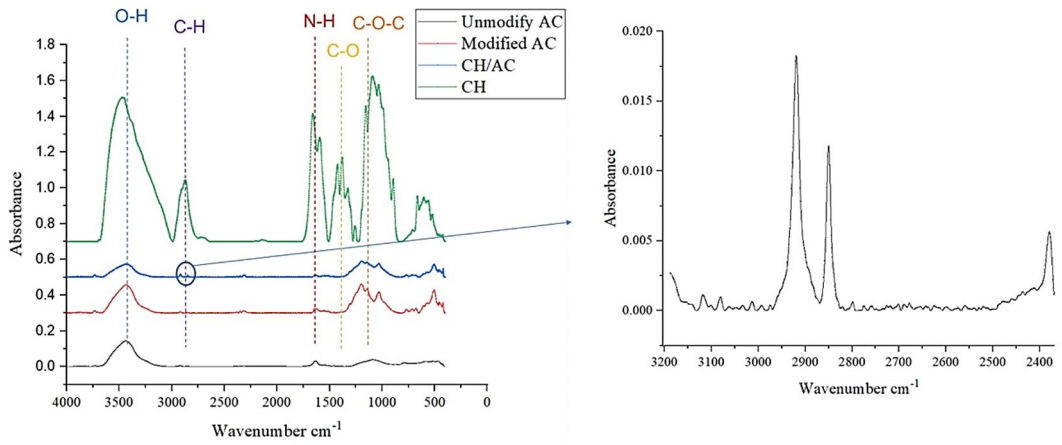


**Fig. 3**. FTIR spectrums of the samples.

## FTIR analysis

The obtained spectrums from FTIR analysis for chitosan, unmodified activated carbon, activated carbon modified with phosphoric acid, and the optimal CH/AC composite samples are depicted in Fig. 3. In the unmodified activated carbon spectrum, the peak at 3437 $cm^{-1}$ indicates O–H stretching vibrations, while the peak at 1089 $cm^{-1}$ is attributed to C–O stretching in acids, alcohols, phenols, ethers, and/or ester groups[19]. In the chitosan spectrum, the peak at 3437 $cm^{-1}$ is associated with O–H and N–H stretching vibrations. The peak at 2871 $cm^{-1}$ corresponds to C–H stretching vibrations, while the peaks at 1659 $cm^{-1}$ and 11,594 $cm^{-1}$ represent N–H bending vibrations, and the peak at 11,088 $cm^{-1}$ indicates C–O–C stretching vibrations[20]. For the activated carbon modified with phosphoric acid spectrum, the peak at 3436 $cm^{-1}$ is linked to O–H stretching of hydroxyl groups and adsorbed water. The peak at 1199 $cm^{-1}$ is attributed to C–O stretching in acids, alcohols, phenols, ethers, and/or ester groups[21]. However, assignment in this region is challenging due to overlapping adsorption bands. The peak at 1200 –1190 $cm^{-1}$ may also be assigned to the P=O stretching mode of the hydrogen bond, O–C stretching vibrations in the P–O–C (aromatic) bond, and P=OOH. Additionally, the peak at 1100 $cm^{-1}$ was attributed to the ionized P–O- bond in acid phosphate esters and the symmetric vibration in the P–O–P chain[22,23]. In the CH/AC composite spectrum, the presence of peaks at 2918 $cm^{-1}$ and 2850 $cm^{-1}$, related to C–H stretching vibrations, and the peak at 1641 $cm^{-1}$, associated with N–H bending vibrations, confirms the successful coverage of chitosan on activated carbon[24].

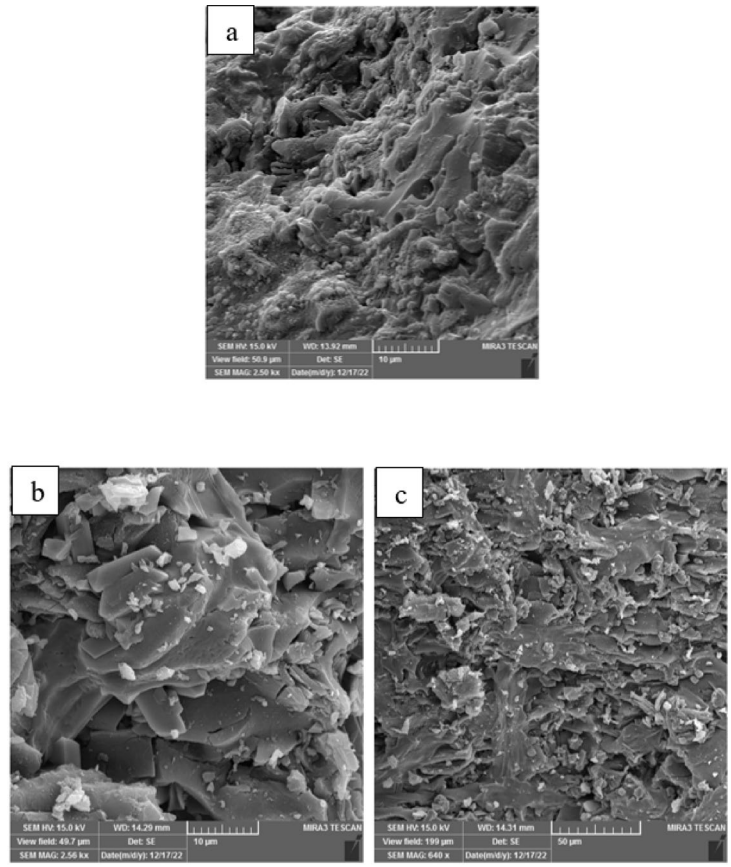


**Fig. 4**. SEM images of (**a**) activated carbons modified with $H_3PO_4$, (**b**, **c**) CH/AC composite in different magnifications.

| Sample | $S_{BET}$ ($m^2$/g) | $V_{tot}$ ($cm^3$/g) | $D_n$ (nm) |
|---|---|---|---|
| CH | 13.71 | 0.02 | 6.47 |
| Modified AC | 791.86 | 0.29 | 2.13 |
| AC/CH composite | 610.31 | 0.37 | 2.08 |

**Table 2**. Physical surface characteristics of adsorbents.

## Surface morphology

Surface characteristics of the activated carbon modified with phosphoric acid and the optimal CH/AC composite samples were examined through FE-SEM analysis. Surface morphology of the activated carbon modified with phosphoric acid shown in Fig. 4a, reveals an irregular, heterogeneous, and porous structure with clearly identifiable pores. The use of phosphoric acid as a cleansing agent aids in the removal of excess material and also cleaning the pores. FE-SEM images illustrate the presence of tunnel-like structures with varying sizes on the activated carbon. These pores serve as primary conduits for accessing the micropores on the inner surface of the activated carbon from the outer surface. The pores on the carbon surfaces appear to be formed by the evaporation of the activating agent, phosphoric acid in this study, leaving behind the space previously occupied by the activating agent. Figure 4b, c demonstrate the FE-SEM results of the CH/AC composite. As can be seen, formation of the almost regular layers on the carbon surface is a proof of the successful coating of activated carbon by chitosan[15,25].

## BET analysis

The results of the BET analysis are shown in Table 2. As can be seen, the specific surface area of the CH/AC composite increased compared to the specific surface area of chitosan itself, but decreased compared to activated carbon, which is probably due to the filling of the carbon pores by chitosan.

The nitrogen adsorption/desorption isotherm for the CH/AC composite is shown in Fig. 5a. The isotherm curve, classified as type I with hysteresis type H1 based on IUPAC, indicates the presence of micropores and cylindrical cavities in the adsorbent. In addition, the average pore diameter of CH, modified AC and CH/AC composite were 6.47 nm, 2.13 nm, and 2.08 nm, respectively. Furthermore, Fig. 5b illustrates the pore size

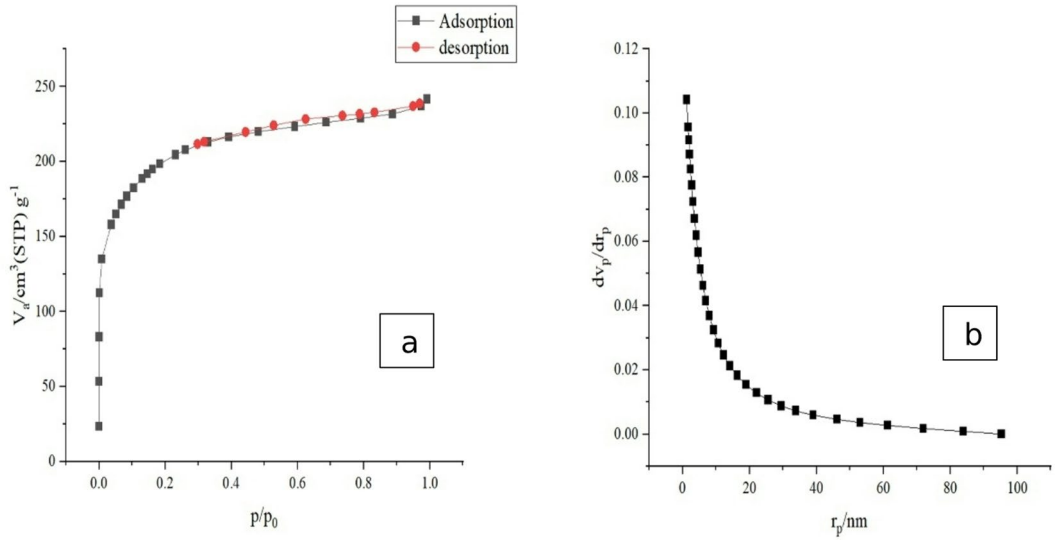


**Fig. 5**. $N_2$ adsorption/desorption isotherm of CH/AC composite (**a**), BJH pore size and area distributions of CH/AC composite (**b**).

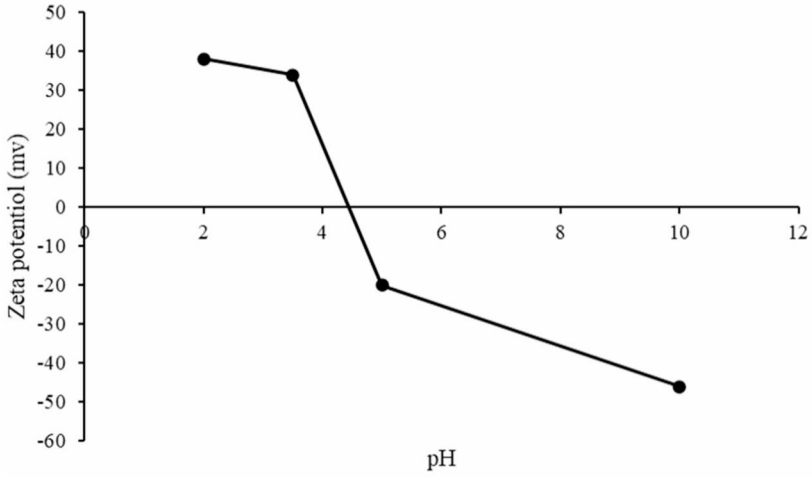


**Fig. 6**. Zeta Potential analysis of CH/AC composite.

distribution of the CH/AC composite according to the BJH method. The distribution of points suggests that the majority of pore radius fall within the range of less than 20 nm[26,27].

## Zeta potential analysis

Figure 6 shows the results of zeta potential analysis. As can be seen, the pH of point zero charge of the composite was found to be 4.4. This means its surface charge is negative above pH = 4.4, and the absolute value gradually increases with increasing solution pH from 4 to 12. CH/AC has a positive charge at pH lower than 4.4. As the pH increases, the charge level becomes negative. This phenomenon can be attributed to the state changes of pH-dependent groups such as carboxyl and hydroxyl groups. In other words, it can be said that the carboxyl group is protonated in acidic conditions, while as the pH increases it is deprotonated, leading to decrease in the zeta potential. Considering that the pollutant used in this work is cationic, in order to improve the performance of the adsorbent in the adsorption process, it is necessary to conduct operational tests at pHs higher than the isoelectric point (pH zero point). According to the Fig. 6, in these areas of pH, the surface charge of the adsorbent is negative, which can have a favorable effect on the adsorption process through the electrostatic adsorption mechanism[28,29].

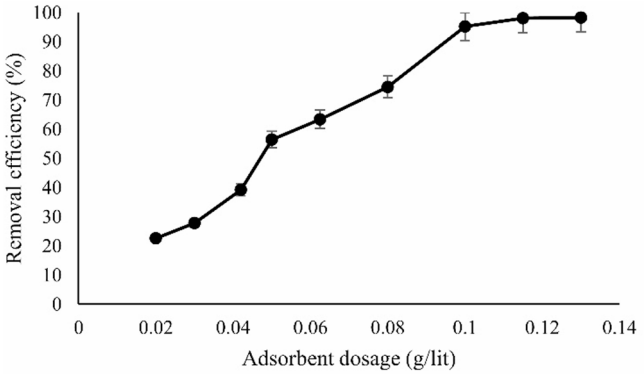


**Fig. 7**. Effect of adsorbent concentration on MB removal by CH/AC composite (initial MB concentration = 30 ppm, contact time = 60 min, shaking speed = 300 rpm, and temperature = 25 °C).

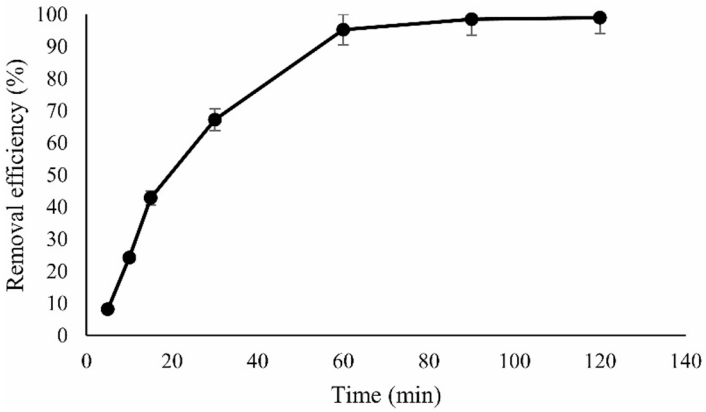


**Fig. 8**. Effect of contact time on MB removal by CH/AC composite (initial MB concentration = 30 ppm, adsorbent dose = 0.1 g, shaking speed = 300 rpm, and temperature = 25 °C).

## Adsorption experiments

*Effect of adsorbent dose*

The influence of adsorbent dosage was examined by altering it while maintaining other parameters such as initial concentration, pH, and time constant. The findings indicate that the efficiency of MB dye increased from 0.05 to 0.1, with no significant change thereafter (Fig. 7). Generally, the removal efficiency of pollutants increases with the rise in adsorbent dose due to the direct increase of surface adsorption sites. An increased adsorbent dose results in a lower ratio of pollutant molecules to empty space, facilitating improved movement and distribution of pollutant molecules on the adsorbent's surface with minimal energy required for their adsorption. Consequently, pollutant adsorption occurs more rapidly, while the adsorption capacity decreases with increasing adsorbent dose. Further increase in adsorbent dose did not notably enhance the process efficiency. As the quantity of adsorbent increases, particularly at higher doses, the number of active sites also increases[30,31].

*Effect of contact time*

In order to examine the progression of the adsorption phenomenon over time, experiments were conducted by maintaining constant all the relevant parameters affecting the adsorption level while varying the duration of the process. As shown in Fig. 8, the adsorption process exhibits rapid progression within the initial 30 min, followed by a gradual deceleration until reaching completion at the 60 min. Consequently, the yield remains relatively constant beyond this point. As a result, the 60 min was identified as the equilibrium time for adsorption, and all analyses of MB adsorption were conducted at this duration.

*Effect of initial MB concentration*

The concentration of the initial dye is considered a crucial factor in the adsorption process. Various studies have indicated that as the dye concentration increases, the adsorption efficiency decreases due to the saturation of active sites on the adsorbent surface. Impact of the initial concentration on the adsorption of MB dye, in relation to removal efficiency is illustrated in Fig. 9. As shown in the figure, when the initial concentration of MB was increased from 10 to 100 ppm, the efficiency of color removal decreased, which may be related to active site occupancy[32].

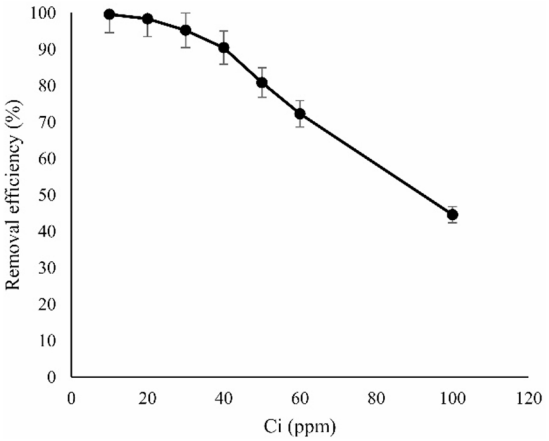


**Fig. 9**. Effect of initial MB concentration on MB removal by CH/AC composite (contact time = 60 min, adsorbent dose = 0.1 g, shaking speed = 300 rpm, and temperature = 25 °C).

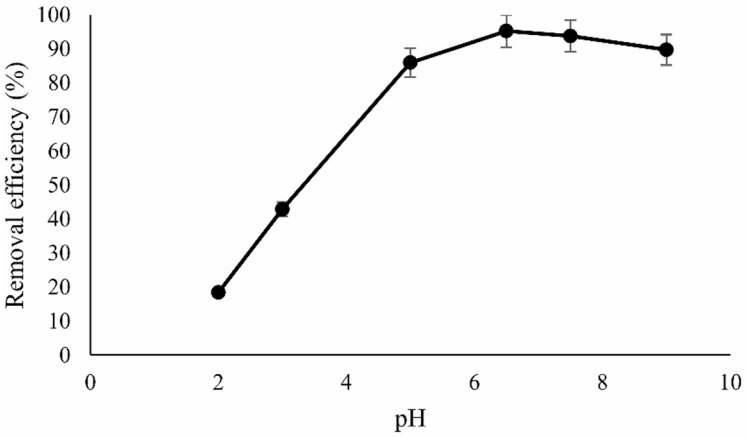


**Fig. 10**. Effect of Solution pH versus MB removal of CH/AC composite (initial MB concentration = 30 ppm, contact time = 60 min, adsorbent dose = 0.1 g, shaking speed = 300 rpm, and temperature = 25 °C).

*Effect of solution pH*

Generally, the pH of solution significantly influences the adsorption capacity due to its impact on the degree of ionization and also surface properties of the adsorbent. In the point of zero charge ($pH_{zpc}$), the adsorbent surface is neutral. At pH below the $pH_{zpc}$, the surface becomes positive, and above it, the surface becomes negative[33,34]. The $pH_{zpc}$ for the synthesized composite was determined 4.4 through zetapotential analysis. This indicates that the adsorbent surface becomes negative in environments with a pH higher than 4.4 and positive in environments with a pH lower than 4.4. The impact of pH changes in the range of 3 to 9 on the removal efficiency of MB dye was also investigated. The results of the effect of pH on the adsorption efficiency of MB dye are illustrated in Fig. 10. The findings demonstrate that the removal efficiency of MB increases as the pH rises from 4 to 9. At pH levels below 4.4, $H^+$ competes with the MB cationic dye as the dominant species, leading to reduced adsorption of MB molecules on the adsorbent surface. Conversely, at pH levels above 4.4, there is no competition between $OH^-$ and MB due to the repulsion of $OH^-$ by the negative charge of the adsorbent surface.

*Adsorption isotherms*

To calculate the maximum equilibrium adsorption capacity, the experimental data were fitted with the Langmuir and Freundlich isotherm models. From the obtained results (Fig. 11), the Langmuir model shows the best fit. This conclusion also is supported by the parameters documented in Table 3. Generally, the Langmuir model describes the monolayer adsorption of adsorbate on a homogeneous adsorbent surface[25]. The results suggest that the adsorption of MB dye occurred as a result of the presence of functional groups serving as active adsorption sites. Additionally, the monolayer adsorption can be attributed to covalent bonds (electron exchange) between the MB dye and the protonated amine and hydroxyl groups of chitosan on the adsorbent surface[35]. Furthermore, the maximum adsorption capacity (22.52 mg/g) obtained from the Langmuir model aligns well with the experimentally determined value (22.31 mg/g).

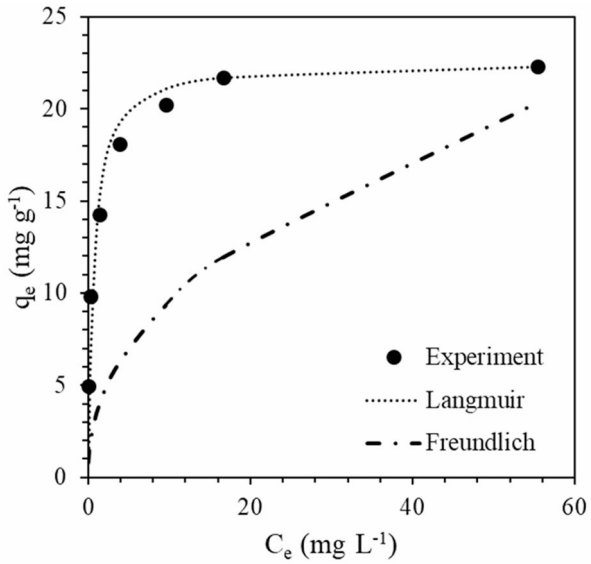


**Fig. 11**. Comparison of adsorption isotherm models.

| Adsorption isotherm | Parameter | Value |
|---|---|---|
| Langmuir | $q_m$ (mg/g) | 22.522 |
| | $K_L$ (L/mg) | 1.515 |
| | $R^2$ | 0.987 |
| Freundlich | $K_F$ (mg/g) $(L/mg)^{1/n}$ | 3.443 |
| | N | 2.526 |
| | $R^2$ | 0.647 |

**Table 3**. Adsorption parameters of Langmuir and Freundlich isotherm models.

| Kinetic model | Parameter | Value |
|---|---|---|
| PFO | $q_e$ (mg. $g^{-1}$) | 15.641 |
| | k1 ($min^{-1}$) | 0.033 |
| | $R^2$ | 0.982 |
| PSO | $q_e$ (mg. $g^{-1}$) | 19.841 |
| | k2 ($g.mg^{-1}$. $min^{-1}$) | 0.001 |
| | $R^2$ | 0.995 |

**Table 4**. Kinetic analysis results of MB adsorption by CH/AC composite.

*Adsorption kinetics*

In order to investigate the adsorption kinetics governing the system during removal of MB process, pseudo-first-order and pseudo-second-order kinetic models were employed. The obtained results are presented in Table 4. Upon comparison of the results, it is evident that the pseudo-second-order kinetic model, with $R^2$ value of 0.995 and $q_e$ value of 19.841, provides the most favorable fit for the adsorption of MB dye. Consequently, it can be inferred that chemical adsorption serves as the governing mechanism for the adsorption of MB dye by the synthesized adsorbent. The outcomes fitting of the experimental data with kinetic models are depicted in Fig. 12.

## Stability of the synthesized adsorbent

The obtained results from the stability analysis of different samples are given in Table 5. The results clearly show that the color removal percentage of activated carbon modified with phosphoric acid is higher than the other samples. According to the FTIR analysis, this finding can be attributed to the presence of a greater variety of functional groups in this sample. However, this sample has challenges in terms of separation and collection after the adsorption process.

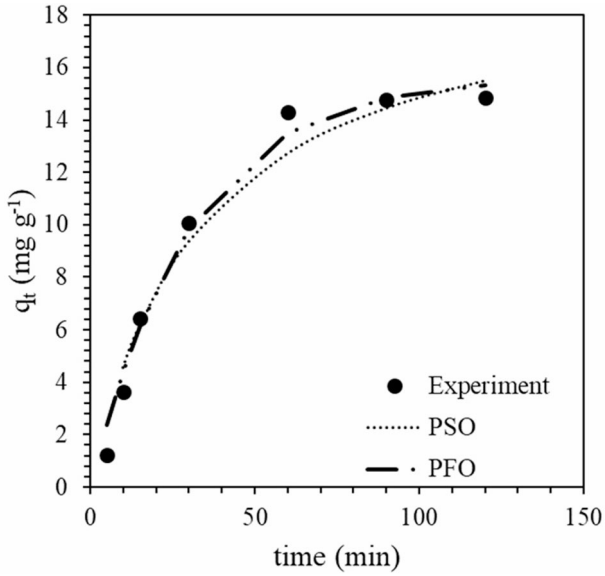


**Fig. 12**. Kinetic modeling of MB adsorption onto CH/AC composite (initial MB concentration = 30 ppm, contact time = 60 min, dose = 0.1 g, shaking speed = 300 rpm and temperature = 25 °C).

| Sample | Removal efficiency |
|---|---|
| Unmodified activated carbon | 88.75 |
| Activated carbon modified with phosphoric acid | 94.51 |
| Chitosan | 45.76 |
| CH/AC composite | 59.46 |

**Table 5**. Comparison of adsorption capacity of samples.

| Sample | Percentage of adsorbent crushing after the adsorption process |
|---|---|
| Unmodified activated carbon | 21.15 |
| Activated carbon modified with phosphoric acid | 28.84 |
| CH/AC composite | 1.92 |

**Table 6**. Comparison of percentage of adsorbent crushing after the adsorption process.

The results of strength and stability of the samples after MB adsorption process are presented in Table 6. According to the findings, it is evident that the CH/AC composite modified with phosphoric acid demonstrates better mechanical strength compared to the other samples.

As mentioned earlier, the aim of this project was to synthesize a stable adsorbent that can be easily collected from the aqueous environment after adsorption process. Adsorbent stability can be defined in two ways: chemical resistance and mechanical strength. The chemical resistance of the synthesized adsorbent refers to the reduction of chitosan dissolution and degradation of the adsorbent in the solution. Also, the mechanical strength refers to the increase in the stability of the adsorbent against erosion caused by agitation and collision of particles with each other and with the container wall during the adsorption process.

It can be clearly seen in Fig. 13 that the amount of powder collected at the bottom of the CH/AC composite container after centrifugation is significantly less than the rest of the samples, which is an indication of the high stability of the adsorbent in the adsorption environment. The synthesized composite exhibits higher resistance in terms of physical and chemical stability compared to activated carbon and chitosan. This can be attributed to interactions with amino and hydroxyl groups. However, due to the participation of active functional groups in these bonds to increase the stability of the adsorbent, the adsorption capacity of the composite decreases.

## Comparison with other adsorbents

The effectiveness of the adsorbents synthesized in this work and other studies under different conditions for the removal of MB was evaluated. According to the results presented in Table 7, the CH/AC composite showed superior MB removal performance compared to many other adsorbents documented in the existing literature. Therefore, the CH/AC composite shows potential as a viable option for the effective removal of MB.

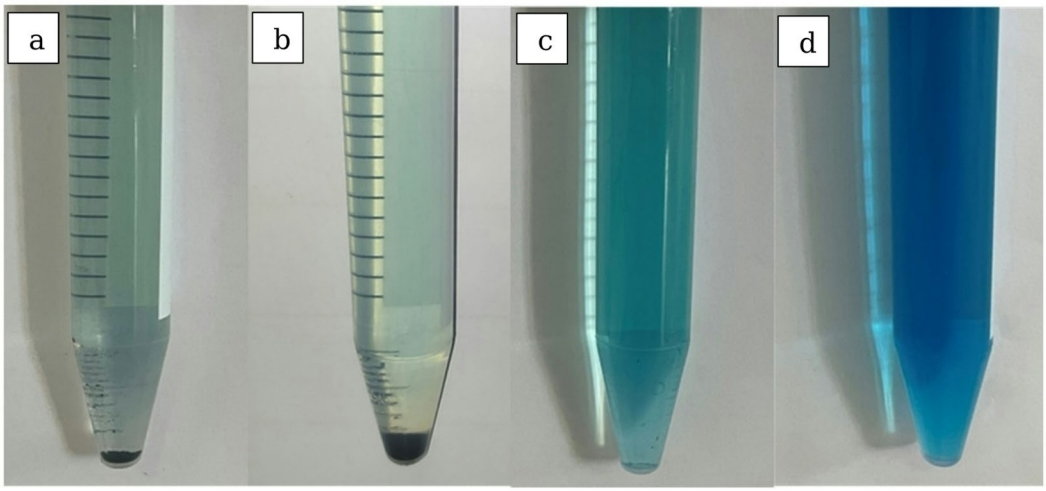


**Fig. 13**. Comparison of samples stability after MB adsorption process: (**a**) Unmodified activated carbon, (**b**) Activated carbon modified with $H_3PO_4$, (**c**) CH/AC composite, (**d**) original color before adsorption process.

| Adsorbents | $q_{max}$ (mg. $g^{-1}$) | pH | Time (min) | Temp (°C) | Isotherm | Reference |
|---|---|---|---|---|---|---|
| Activated fly ash (AFSH) | 14.28 | 9 | 100 | 20 | Freundlich | Banerjee et al.[36] |
| Magnetic chitosan/organic rectorite | 24.69 | 6 | 60 | 25 | Langmuir | Zheng et al.[37] |
| Magnetic activated carbon | 2.046 | 10 | 120 | 25 | Freundlich | Abuzerr et al.[38] |
| $Fe_3O_4$-$TiO_2$ NPs/methyltrimethoxysilane | 11.57 | 9 | – | 25 | Langmuir | Alizadeh et al.[39] |
| $H_2SO_4$ crosslinked magnetic chitosan nanocomposite beads | 20.408 | 12 | 30 | – | Langmuir | Mustafa et al.[40] |
| Modified $TiO_2$ | 9.800 | 6 | – | 25 | Langmuir | Mohammadi et al.[41] |
| Activated lignin-chitosan pellets | 36.25 | 7 | – | 20 | Langmuir | Albadarin et al.[42] |
| Graphene oxide/chitosan/$Fe_3O_4$ | 30.10 | 10.5 | – | – | Langmuir | Tran et al.[43] |
| Graphene oxide/$TiO_2$ | 26.30 | 6.8 | – | 25 | Langmuir | Nguyen et al.[44] |
| $TiO_2$/Carbon | 25.73 | 6 | – | 55 | Langmuir | Simonetti et al.[45] |
| Chitosan/Activated Carbon | 22.52 | 6.5 | 60 | 25 | Langmuir | This work |

**Table 7**. Adsorption performance of MB via different adsorbents.

## Adsorption mechanism

The adsorption process of MB on the CH/AC composite is complicated because several factors are involved that affect the interaction between the adsorbent and the adsorbate. Various possible interactions for the adsorption of methylene blue on the CH/AC composite are shown in Fig. 14. Basically, in the aqueous solutions there is a strong electrostatic interaction between the charged surfaces of the adsorbent and dye molecules. The interaction between activated sites of carbon and MB includes electrostatic attraction, hydrogen bonding, π–π stacking, and hydrophobic interactions[28]. As described, changes in the pH of the solution have a direct impact on the dye adsorption on the composite. The pH of the solution affects the binding sites and chemical interaction by changing the ionization state of the functional groups on the surface of the CH/AC composite, and it has been shown that the removal rate of dyes increases with increasing pH due to hydroxyl increases protonation. In general, acidic functional groups increase the adsorption capacity[46,47]. By referring to the FTIR analysis of the synthesized composite, the presence of various acidic functional groups in the adsorbent structure is confirmed. In addition, the specific surface area plays a crucial role in the adsorption process. The results of BET analysis show that the synthesized adsorbent has a suitable specific surface area that favors the adsorption of MB molecules.

## Conclusions

Activated carbon-based chitosan composite adsorbent was synthesized to treat simulated MB dye wastewater. The results indicated the successful synthesis of CH/AC composite adsorbent with a unique easy separation capability after adsorption process. In spite of higher stability of the synthesized composite, it showed lower adsorption capacity compared to unmodified others due to presence of amino and hydroxyl functional groups in chitosan. However, the desired adsorption capacity of the composite for MB comparing to the other studies

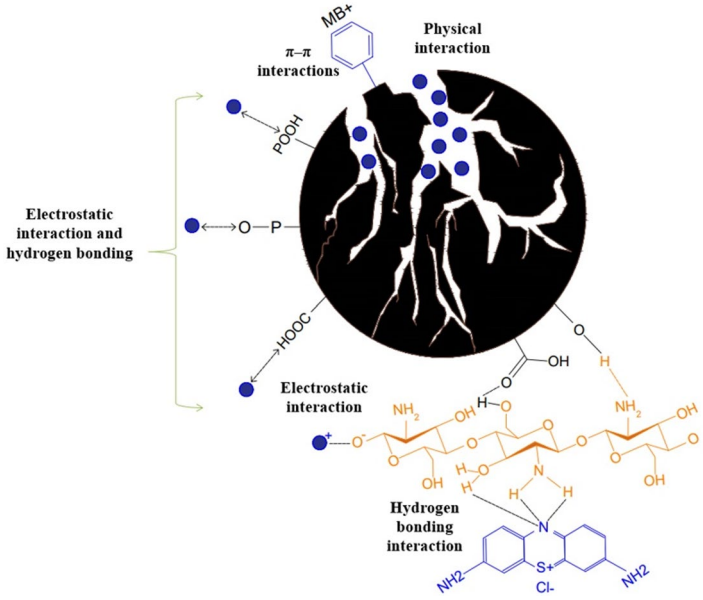


**Fig. 14**. Schematic diagram of the possible mechanism for the removal of MB by the CH/AC composite.

is due to the combination of large specific surface area and high concentration of acidic functional groups. The important features of this modified adsorbent are the possibility of easy separation of adsorbent particles from the solution by using a strainer, which helps to facilitate the recovery process of the adsorbent as well as its reuse. According to the favorable results obtained from this study regarding the removal of MB cationic pollutant, there is a hope that this adsorbent can be used for the removal of other cationic pollutants such as heavy metals with the possibility of easy separation without the need for a centrifuge device, after the adsorption process.

## Data availability

Data is provided within the manuscript .

Received: 1 June 2025; Accepted: 23 September 2025
Published online: 29 October 2025

## 6. References

1. Lim, J. Y. et al. Recent trends in the synthesis of graphene and graphene oxide based nanomaterials for removal of heavy metals—A review. *J. Ind. Eng. Chem.* **66**, 29–44 (2018).
2. Kumar, P. S., Varjani, S. J. & Suganya, S. Treatment of dye wastewater using an ultrasonic aided nanoparticle stacked activated carbon: kinetic and isotherm modelling. *Bioresour. Technol.* **250**, 716–722 (2018).
3. Huang, Y. et al. Preparation of porous graphene/carbon nanotube composite and adsorption mechanism of methylene blue. *SN Appl. Sci.* **1** (1), 37 (2019).
4. Hamad, H. N. & Idrus, S. Recent developments in the application of bio-waste-derived adsorbents for the removal of methylene blue from wastewater: a review. *Polymers* **14** (4), 783 (2022).
5. Sheth, Y., Dharaskar, S., Khalid, M. & Sonawane, S. An environment friendly approach for heavy metal removal from industrial wastewater using Chitosan based biosorbent: A review. *Sustain. Energy Technol. Assess.* **43**, 100951 (2021).
6. Banerjee, S. & Chattopadhyaya, M. Adsorption characteristics for the removal of a toxic dye, tartrazine from aqueous solutions by a low cost agricultural by-product. *Arab. J. Chem.* **10**, S1629–S1638 (2017).
7. Ding, B. et al. Nitrogen-enriched carbon nanofiber aerogels derived from marine Chitin for energy storage and environmental remediation. *ACS Sustain. Chem. Eng.* **6** (1), 177–185 (2018).
8. Negarestani, M. et al. Preparation of polypyrrole-functionalized recycled cotton fiber as a renewable and eco-friendly cellulose-based adsorbent for water decolorization: comprehensive batch and fixed-bed column study. *Surf. Interfaces.* **48**, 104360 (2024).
9. Negarestani, M. et al. Preparation of Sisal fiber/polyaniline/bio-surfactant rhamnolipid-layered double hydroxide nanocomposite for water decolorization: kinetic, equilibrium, and thermodynamic studies. *Sci. Rep.* **13** (1), 11341 (2023).
10. Negarestani, M. et al. Natural and environmentally friendly rhamnolipid functionalized Luffa fibers for adsorptive removal of pharmaceutical contaminant: batch and fixed-bed column studies. *Chem. Eng. Sci.* **299**, 120552 (2024).
11. Muzzarelli, R. A. et al. Current views on fungal Chitin/chitosan, human Chitinases, food preservation, glucans, pectins and inulin: A tribute to Henri Braconnot, precursor of the carbohydrate polymers science, on the Chitin bicentennial. *Carbohydr. Polym.* **87** (2), 995–1012 (2012).
12. Elwakeel, K. Z. et al. Synthesis of chitosan@ activated carbon beads with abundant amino groups for capture of Cu (II) and cd (II) from aqueous solutions. *J. Polym. Environ.* **26**, 3590–3602 (2018).
13. Wei, Q. et al. Preparation and electrochemical performance of orange Peel based-activated carbons activated by different activators. *Colloids Surf., A.* **574**, 221–227 (2019).
14. Fatombi, J. K. et al. Adsorption of Indigo Carmine from aqueous solution by Chitosan and Chitosan/activated carbon composite: kinetics, isotherms and thermodynamics studies. *Fibers Polym.* **20**, 1820–1832 (2019).
15. Sharififard, H., Nabavinia, M. & Soleimani, M. Evaluation of adsorption efficiency of activated carbon/chitosan composite for removal of cr (VI) and cd (II) from single and bi-solute dilute solution. *Adv. Environ. Technol.* **2** (4), 215–227 (2017).

16. Yunus, Z. M. et al. Advanced methods for activated carbon from agriculture wastes; a comprehensive review. *Int. J. Environ. Anal. Chem.* **102** (1), 134–158 (2022).
17. Lopez, E. et al. Adsorbent properties of red mud and its use for wastewater treatment. *Water Res.* **32** (4), 1314–1322 (1998).
18. Liu, L., Li, Y. & Fan, S. Preparation of KOH and H3PO4 modified Biochar and its application in methylene blue removal from aqueous solution. *Processes* **7** (12), 891 (2019).
19. Yakout, S. & El-Deen, G. S. Characterization of activated carbon prepared by phosphoric acid activation of Olive stones. *Arab. J. Chem.* **9**, S1155–S1162 (2016).
20. Leceta, I. et al. Characterization and antimicrobial analysis of chitosan-based films. *J. Food Eng.* **116** (4), 889–899 (2013).
21. Zawadzki, J. Infrared spectroscopy in surface chemistry of carbons. *Chem. Phys. Carbon*. **21**, 147–380 (1989).
22. Puziy, A. et al. Synthetic carbons activated with phosphoric acid: I. Surface chemistry and ion binding properties. *Carbon* **40** (9), 1493–1505 (2002).
23. Bourbigot, S. et al. Carbonization mechanisms resulting from intumescence-part II. Association with an ethylene terpolymer and the ammonium polyphosphate-pentaerythritol fire retardant system. *Carbon* **33** (3), 283–294 (1995).
24. Hydari, S., Sharififard, H., Nabavinia, M. & reza Parvizi, M. A comparative investigation on removal performances of commercial activated carbon, Chitosan biosorbent and Chitosan/activated carbon composite for cadmium. *Chem. Eng. J.* **193**, 276–282 (2012).
25. Oginni, O. et al. Effect of one-step and two-step H3PO4 activation on activated carbon characteristics. *Bioresource Technol. Rep.* **8**, 100307 (2019).
26. Yuan, Y. et al. A facile hydrothermal synthesis of a MnCo2O4@ reduced graphene oxide nanocomposite for application in supercapacitors. *Chem. Lett.* **43** (1), 83–85 (2014).
27. Fu, Y., Chen, H., Sun, X. & Wang, X. Combination of Cobalt ferrite and graphene: high-performance and recyclable visible-light photocatalysis. *Appl. Catal. B.* **111**, 280–287 (2012).
28. Han, Q. et al. High adsorption of methylene blue by activated carbon prepared from phosphoric acid treated Eucalyptus residue. *Powder Technol.* **366**, 239–248 (2020).
29. Zeng, G. et al. Adsorptive removal of cr (VI) by sargassum horneri–based activated carbon coated with Chitosan. *Water Air Soil Pollut.* **231**, 1–12 (2020).
30. Nayeri, D. & Mousavi, S. A. Dye removal from water and wastewater by nanosized metal oxides-modified activated carbon: a review on recent researches. *J. Environ. Health Sci. Eng.* **18** (2), 1671–1689 (2020).
31. Mashkoor, F., Nasar, A., Inamuddin & Asiri, A. M. Exploring the reusability of synthetically contaminated wastewater containing crystal Violet dye using tectona grandis sawdust as a very low-cost adsorbent. *Sci. Rep.* **8** (1), 8314 (2018).
32. Etim, U., Umoren, S. & Eduok, U. Coconut Coir dust as a low cost adsorbent for the removal of cationic dye from aqueous solution. *J. Saudi Chem. Soc.* **20**, S67–S76 (2016).
33. Malik, V. et al. *Review on adsorptive removal of metal ions and dyes from wastewater using tamarind-based bio-composites. Polym. Bull.*, : pp. 1–36. (2022).
34. Bushra, R. et al. Current approaches and methodologies to explore the perceptive adsorption mechanism of dyes on low-cost agricultural waste: A review. *Microporous Mesoporous Mater.* **319**, 111040 (2021).
35. Wang, J. & Guo, X. Adsorption isotherm models: Classification, physical meaning, application and solving method. *Chemosphere* **258**, 127279 (2020).
36. Banerjee, S., Sharma, G. C., Chattopadhyaya, M. & Sharma, Y. C. Kinetic and equilibrium modeling for the adsorptive removal of methylene blue from aqueous solutions on of activated fly Ash (AFSH). *J. Environ. Chem. Eng.* **2** (3), 1870–1880 (2014).
37. Zeng, L. et al. Chitosan/organic rectorite composite for the magnetic uptake of Methylene blue and Methyl orange. *Carbohydr. Polym.* **123**, 89–98 (2015).
38. Abuzerr, S., Darwish, M. & Mahvi, A. H. Simultaneous removal of cationic methylene blue and anionic reactive red 198 dyes using magnetic activated carbon nanoparticles: equilibrium, and kinetics analysis. *Water Sci. Technol.* **2017** (2), 534–545 (2018).
39. Alizadeh Eslami, P., Kamboh, M. A., Nodeh, H. R., Wan, W. A. & Ibrahim Equilibrium and kinetic study of novel Methyltrimethoxysilane magnetic titanium dioxide nanocomposite for methylene blue adsorption from aqueous media. *Appl. Organomet. Chem.* **32** (6), e4331 (2018).
40. Mustafa, I. Methylene blue removal from water using H2SO4 crosslinked magnetic Chitosan nanocomposite beads. *Microchem. J.* **144**, 397–402 (2019).
41. Mohammadi, A., Aliakbarzadeh, A. & Karimi Methylene blue removal using surface-modified TiO2 nanoparticles: a comparative study on adsorption and photocatalytic degradation. *J. Water Environ. Nanatechnol.* **2** (2), 118–128 (2017).
42. Albadarin, A. B. et al. Activated lignin-chitosan extruded blends for efficient adsorption of methylene blue. *Chem. Eng. J.* **307**, 264–272 (2017).
43. Tran, H. V. et al. Graphene oxide/Fe3O4/chitosan nanocomposite: a recoverable and recyclable adsorbent for organic dyes removal. Application to methylene blue. *Mater. Res. Express*. **4** (3), 035701 (2017).
44. Nguyen, C. H. & Juang, R. S. Efficient removal of methylene blue dye by a hybrid adsorption–photocatalysis process using reduced graphene oxide/titanate nanotube composites for water reuse. *J. Ind. Eng. Chem.* **76**, 296–309 (2019).
45. Simonetti, E. A. N. et al. Carbon and TiO2 synergistic effect on methylene blue adsorption. *Mater. Chem. Phys.* **177**, 330–338 (2016).
46. Ma, Z. W., Zhang, K. N., Zou, Z. J. & Lü, Q. F. High specific area activated carbon derived from Chitosan hydrogel coated tea saponin: One-step Preparation and efficient removal of methylene blue. *J. Environ. Chem. Eng.* **9** (3), 105251 (2021).
47. Ahmad, R. & Ansari, K. Comparative study for adsorption of congo red and methylene blue dye on Chitosan modified hybrid nanocomposite. *Process Biochem.* **108**, 90–102 (2021).

## Author contributions
This research is the result of Fatemeh Ebrahimzadeh's master's thesis under the guidance of me (Dr. Ali Akbari) as the supervisor.

## Funding
not applicable.

## Declarations

## Competing interests
The authors declare no competing interests.

## Ethics and consent to participate
Not applicable.

## Consent for publication
Not applicable.

## Additional information
**Correspondence** and requests for materials should be addressed to A.A.

**Reprints and permissions information** is available at www.nature.com/reprints.

**Publisher's note** Springer Nature remains neutral with regard to jurisdictional claims in published maps and institutional affiliations.